

How Entanglement is Lost: Disentanglement in Unitary Evolution

Enrique P. Blair

*Electrical and Computer Engineering Department
Baylor University
Waco, TX*

Craig S. Lent*

*Department of Electrical Engineering
and Department of Physics
University of Notre Dame Notre Dame, IN
(Dated: March 24, 2017)*

Initially fully-entangled Bell states can become disentangled as a result of interaction with their environment through purely coherent unitary time evolution. We calculate the Mermin and the Clauser-Horne-Shimony-Holt (CHSH) Bell correlation functions for a system of quantum entangled double-dots that interact with local environments. The temporal evolution of the global system, target cells plus environment, is entirely unitary. There is no loss of quantum coherence or quantum information. The vanishing of entanglement follows a Gaussian form and classical correlations emerge that are consistent with local realism. We calculate the characteristic time-scale for disentanglement and demonstrate scaling across different environments and strengths of interaction.

The central feature of quantum mechanics is the existence of a coherent superposition state. The outcome of a measurement of the key properties of such a state cannot be predicted by the physical law, even in principle. Indeed properties of a superposition state do not *have* values until a measurement is made. This fundamental lack of determinism in the physical law was famously unsatisfying to Einstein [1], as well as many since, because of the strong intuitive appeal of local realism—there must be a “fact of the matter” prior to measurement that determines outcomes. Whether the indeterminism of quantum mechanics is fundamental or reflects a deeper determinism that is somehow veiled could be considered a philosophical question until Bell showed how it could be directly tested [2]. He considered a superposition state of a bipartate system whose components could be physically separated. There is no new quantum mechanics in such “entangled” states beyond the principle of superposition, but it makes it possible to probe the fundamental nature of the non-intuitive quantum superposition. By considering correlations between measurements made on each sub-system Bell showed that quantum mechanics is incompatible with local realism and that the question of which is correct could be put to experimental test.

A series of pioneering Bell tests over the last few decades have measured Bell correlation functions for entangled states which violate local realism and confirm the predictions of quantum mechanics. Various “loop holes” through which a hidden determinism could conceivably slip have been closed, one after the other. Until recently, however, they were not all closed in the same experiment. Now several groups [3–6] have demonstrated loop-hole free Bell tests which clearly establish the violation of local realism and thus the fundamental indeterminism of the physical law. Any a successor theory to quantum

mechanics would have to include this feature. Experiments have yet to probe temporal development of the loss of entanglement as separated systems interact with their environments.

Interacting systems entangle, but if entanglement is a basic feature of the world why do we not see it everywhere? Why does it appear to be such a fragile and subtle effect? As with the very successful decoherence theory of Zurek *et al.*, the key is the multiplicity of the interactions with the environment [7]. We would like to see how local realism emerges in time from purely quantum mechanical dynamics as a feature of these environmental interactions.

We consider a model system of two entangled quantum double-dots surrounded by geometrically random environments of similar double-dots, all interacting Coulombically. The geometrical randomness just prevents any artifacts of an ordered system. There is nothing random in the interaction or the dynamics. This system is a useful model for molecular mixed-valence quantum double-dot systems and has the advantage of including a natural and physically realistic coupling mechanism [8]. The initially entangled bipartate system and the full environment are all treated on the same footing, with global unitary time evolution. We then examine two Bell correlation functions, the Mermin [9, 10] and Clauser-Horne-Shimony-Holt (CHSH) [11] functions, and look for the transition to classical (i.e., local realistic) behavior and the time scale on which this happens.

The target double-dot cells labeled A and B are described using a two-state basis composed of states $|\alpha_0^A\rangle = |0_A\rangle$, $|\alpha_1^A\rangle = |1_A\rangle$, $|\alpha_0^B\rangle = |0_B\rangle$, and $|\alpha_1^B\rangle = |1_B\rangle$ in which the electron is fully localized on the bottom (0) or top (1) dot respectively. A fixed charge of $+e/2$ resides at each dot, providing net charge neutrality for

each cell. The two initially entangled double-dots are abruptly moved far apart and then allowed to each interact with a separate environment.

The environment is composed of several similar cells surrounding the target cells. The environmental cells are arranged in a sphere of radius R with the positions on the sphere and the orientation of the double-dots chosen randomly as shown in Fig. 1. Each of the environmental cells, indexed by $k = 1, 2, \dots, N$, is described by a similar two-state basis $|\alpha_0^k\rangle = |0_k\rangle$ and $|\alpha_1^k\rangle = |1_k\rangle$. There are $N/2$ environmental cells surrounding each target cell (N is always chosen to be even). We label individual cell basis states with an integer $m \in [0, 1]$. Target cell basis states are indexed with m_A and m_B , while the k_{th} environmental cell is indexed with m_k .

The electronic configuration associated with a specific environmental basis state can then be referred to using the vector

$$\vec{m} \equiv [m_1, m_2, \dots, m_N]. \quad (1)$$

There are $N_E = 2^N$ such vectors, $[\vec{m}_1, \vec{m}_2, \vec{m}_3, \dots, \vec{m}_{N_E}]$, each representing a specific

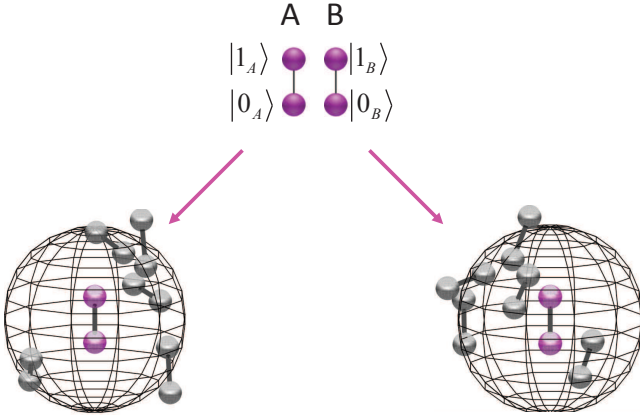


FIG. 1. A pair of entangled quantum double-dots are abruptly separated and interact with local environments. Each pair of spheres represents a double-dot with dot separation a . The basis states for each pair correspond to a 1 (top dot occupied) or 0 (bottom dot occupied). The target pair of double-dots (colored in purple) are prepared in an entangled symmetric Bell state. After abruptly being separated, each interacts with a local environment of similar double dots, randomly positioned and oriented around them in a sphere of radius R . The Coulomb interaction couples the double-dot states and the global system evolves under coherent unitary evolution.

electronic configuration of the environment E .

$$\begin{aligned} \vec{m}_1 &= [0, 0, 0, \dots, 0] \\ \vec{m}_2 &= [1, 0, 0, \dots, 0] \\ \vec{m}_3 &= [0, 1, 0, \dots, 0] \\ \vec{m}_4 &= [1, 1, 0, \dots, 0] \\ &\vdots \\ \vec{m}_{N_E} &= [1, 1, 1, \dots, 1] \end{aligned} \quad (2)$$

The basis states for describing the global system Ω , which includes the two target double dots and the environment, consist of the direct products of the individual cell states.

$$|\Phi_{m_A, m_B, \vec{m}_p}\rangle = |\alpha_{m_A}^A\rangle |\alpha_{m_B}^B\rangle |\alpha_{[\vec{m}_p]_1}^1\rangle |\alpha_{[\vec{m}_p]_2}^2\rangle \dots |\alpha_{[\vec{m}_p]_N}^N\rangle \quad (3)$$

The global state can then be written as a linear combination of these basis states.

$$|\psi(t)\rangle = \sum_{\substack{m_A=0,1 \\ m_B=0,1 \\ p=1,2,\dots,N_E}} c_{m_A, m_B, \vec{m}_p}(t) |\Phi_{m_A, m_B, \vec{m}_p}\rangle \quad (4)$$

The Hamiltonian for the global system, including A , B , and the environment E , is determined only by the electrostatic interaction between cells in the basis state electronic configurations. Let $U_{m_j, m_k}^{j,k}$ be the electrostatic potential energy between the j^{th} cell in state m_j (0 or 1) and the k^{th} cell in state m_k (0 or 1). This energy is given by

$$U_{m_j, m_k}^{j,k} = \frac{P(m_j)P(m_k)e^2}{16\pi\epsilon_o} \left[\frac{1}{r_{0,0}^{j,k}} - \frac{1}{r_{0,1}^{j,k}} - \frac{1}{r_{1,0}^{j,k}} + \frac{1}{r_{1,1}^{j,k}} \right]. \quad (5)$$

where e is the fundamental charge, ϵ_o is the permittivity of free space, $r_{m_j, m_k}^{j,k}$ is the distance between dot m_j in cell j and dot m_k in cell k , and $P(m)$ is the polarization of a cell in state m . $P(1) = +1$ and $P(0) = -1$.

The total electrostatic potential energy of a configuration of target cells in states m_A and m_B , and the environment in the state defined by \vec{m}_p is calculated by simply summing over all interactions between all pairs of cells.

$$E_{m_A, m_B, \vec{m}_p} = \frac{1}{2} \sum_{\substack{j,k=1 \\ j \neq k}} U_{m_i, m_j}^{j,k}. \quad (6)$$

Here the sums over indices i and j are over the cells $[A, B, 1, 2, \dots, N]$, that is, including both target and environmental cells.

In this model there is no tunneling between dots within the cell; we are interested in the entanglement of the phase degrees of freedom rather than electron transfer

effects which have been studied elsewhere using a similar model [12]. The Hamiltonian for the global system is then diagonal in the basis states define by Eq. (3) is:

$$\hat{H} = \sum_{m_A, m_B, p} |\Phi_{m_A, m_B, \vec{m}_p}\rangle E_{m_A, m_B, \vec{m}_p} \langle \Phi_{m_A, m_B, \vec{m}_p}|. \quad (7)$$

We can characterize the strength of the interaction between each target cell and its local environment by the electrostatic energy to flip cell A or B from 0 to 1 with the environment in state \vec{m}_p .

$$E_{A, \vec{m}_p}^{\text{flip}} \equiv E_{1, m_B, \vec{m}_p} - E_{0, m_B, \vec{m}_p} \quad (8)$$

$$E_{B, \vec{m}_p}^{\text{flip}} \equiv E_{m_A, 1, \vec{m}_p} - E_{m_A, 0, \vec{m}_p} \quad (9)$$

Let the root-mean-square of the flip energies over all the electronic configurations of the local environmental basis states be $E_{\text{RMS}}^{\text{flip}}(A/B)$. A characteristic time can then be defined for each of the separated systems and the system as a whole:

$$\tau_{A,E} = h/E_{\text{RMS}}^{\text{flip}}(A), \quad \tau_{B,E} = h/E_{\text{RMS}}^{\text{flip}}(B), \quad \tau_E = \sqrt{\tau_{A,E} \tau_{B,E}}. \quad (10)$$

This characteristic time τ_E depends on the details of the geometrically random orientation and positions of the environmental cells.

The density operator for the global system is defined from (4) by

$$\begin{aligned} \hat{\rho}_\Omega(t) &= |\psi(t)\rangle \langle \psi(t)| \\ &= \sum_{\substack{m_A, m'_A \\ m_B, m'_B \\ p, p'}} c_{m'_A, m'_B, \vec{m}_p}^* c_{m_A, m_B, \vec{m}_p} |\Phi_{m_A, m_B, \vec{m}_p}\rangle \langle \Phi_{m'_A, m'_B, \vec{m}_p}| \end{aligned} \quad (11)$$

We solve for the global system density matrix as a function of time using the quantum Liouville equation.

$$\hat{\rho}_\Omega(t) = e^{-i\frac{\hat{H}}{\hbar}t} \hat{\rho}_\Omega(0) e^{+i\frac{\hat{H}}{\hbar}t} \quad (12)$$

This time evolution is exact within the model and the global system described by $\hat{\rho}_\Omega$ is always in a pure state.

The target double-dots A and B are initially in the symmetric entangled Bell state.

$$|\psi^{AB}(0)\rangle = [|\alpha_1^A\rangle |\alpha_1^B\rangle + |\alpha_0^A\rangle |\alpha_0^B\rangle] / \sqrt{2} \quad (13)$$

with the corresponding density operator.

$$\hat{\rho}^{AB}(0) = |\psi^{AB}(0)\rangle \langle \psi^{AB}(0)| \quad (14)$$

The initial state of the k_{th} environmental cell is an unpolarized state

$$|\psi_k(0)\rangle = e^{i\theta_k} (|0_k\rangle + e^{i\phi_k} |1_k\rangle) / \sqrt{2}, \quad (15)$$

where the phases θ_k and ϕ_k are chosen randomly.

We take the initial state of the density operator to be a direct product state of the entangled system AB and the environment.

$$\begin{aligned} \hat{\rho}_\Omega(0) &= \hat{\rho}^{AB}(0) \otimes [|\psi_1(0)\rangle \langle \psi_1(0)|] \otimes [|\psi_2(0)\rangle \langle \psi_2(0)|] \\ &\quad \cdots \otimes [|\psi_N(0)\rangle \langle \psi_N(0)|]. \end{aligned} \quad (16)$$

For each subsystem A and B we can define operators in the space spanned by the local basis vectors $|\alpha_0\rangle$ and $|\alpha_1\rangle$. In this basis we define the rotation operator \hat{R} and three sets of rotated basis function.

$$\begin{aligned} \hat{R}(\theta) &= \cos(\theta) [|\alpha_1\rangle \langle \alpha_1| + |\alpha_0\rangle \langle \alpha_0|] \\ &\quad + \sin(\theta) [|\alpha_0\rangle \langle \alpha_1| - |\alpha_1\rangle \langle \alpha_0|] \end{aligned} \quad (17)$$

$$\begin{aligned} |u_0\rangle &= \hat{R}(\theta_1) |\alpha_0\rangle & |u_1\rangle &= \hat{R}(\theta_1) |\alpha_1\rangle \\ |v_0\rangle &= \hat{R}(\theta_2) |\alpha_0\rangle & |v_1\rangle &= \hat{R}(\theta_2) |\alpha_1\rangle \\ |w_0\rangle &= \hat{R}(\theta_3) |\alpha_0\rangle & |w_1\rangle &= \hat{R}(\theta_3) |\alpha_1\rangle \end{aligned} \quad (18)$$

For the Mermin correlation function we choose $[\theta_1, \theta_2, \theta_3] = [0^\circ, 60^\circ, 120^\circ]$. For each subsystem A and B a particular basis set corresponding to one of these angles is randomly chosen and a projective measurement is made. The projection operators corresponding to measurements of the properties U , V , or W , can then be defined which act on one or the other subsystem.

$$\begin{aligned} \hat{P}_U^0 &= |u_0\rangle \langle u_0| & \hat{P}_U^1 &= |u_1\rangle \langle u_1| \\ \hat{P}_V^0 &= |v_0\rangle \langle v_0| & \hat{P}_V^1 &= |v_1\rangle \langle v_1| \\ \hat{P}_W^0 &= |w_0\rangle \langle w_0| & \hat{P}_W^1 &= |w_1\rangle \langle w_1| \end{aligned} \quad (19)$$

Each of these operators has eigenvalues 0 and 1, which would result from a measurement of any of the three properties (U, V, W) on either subsystem A or B . We define the correlation operators

$$\begin{aligned} \hat{P}_{same}^{UV}(A, B) &= \hat{P}_U^0(A) \otimes \hat{P}_V^0(B) + \hat{P}_U^1(A) \otimes \hat{P}_V^1(B) \\ \hat{P}_{same}^{UW}(A, B) &= \hat{P}_U^0(A) \otimes \hat{P}_W^0(B) + \hat{P}_U^1(A) \otimes \hat{P}_W^1(B) \\ \hat{P}_{same}^{VW}(A, B) &= \hat{P}_V^0(A) \otimes \hat{P}_W^0(B) + \hat{P}_V^1(A) \otimes \hat{P}_W^1(B). \end{aligned} \quad (20)$$

The operator $\hat{P}_{same}^{UV}(A, B)$, for example, corresponds to a measurement of U on one subsystem and V on the other, both yielding the same result (both 0 or both 1). The statistics of such events can be gathered experimentally and compared to theoretical prediction. The Mermin correlation function is then defined as follows:

$$S_{\text{Mermin}} = \langle \hat{P}_{same}^{UV}(A, B) + \hat{P}_{same}^{UW}(A, B) + \hat{P}_{same}^{VW}(A, B) \rangle. \quad (21)$$

Local realism requires that each subsystem A and B have values that determine the results of measurements of properties U , V , and W before the measurement is

made. That assumption yields the Mermin-Bell inequality:

$$S_{\text{Mermin}} \geq 1 \quad (22)$$

for any probability distribution of the property values [10]. If the properties of each subsystem obey local realism and are only classically correlated $S_{\text{Mermin}} = 9/8$. By contrast, the fully entangled Bell state of Eq. (13) yields $S_{\text{Mermin}} = 3/4$ in clear violation of Eq. (22).

We evaluate directly the time-dependent value $S_{\text{Mermin}}(t)$ from the density matrix evolving in time under Eq. (12).

To calculate the CHSH (Clauser, Horne, Shimony, Holt) correlation function [11] we define two basis sets, \mathbf{a} and \mathbf{a}' , for measurement of the A subsystem, and two basis states, \mathbf{b} and \mathbf{b}' , for measurements of the the B subsystem.

$$\begin{aligned} |a_0\rangle &= \hat{R}(\theta_a) |\alpha_0^A\rangle & |a_1\rangle &= \hat{R}(\theta_a) |\alpha_1^A\rangle \\ |a'_0\rangle &= \hat{R}(\theta_{a'}) |\alpha_0^A\rangle & |a'_1\rangle &= \hat{R}(\theta_{a'}) |\alpha_1^A\rangle \\ |b_0\rangle &= \hat{R}(\theta_b) |\alpha_0^B\rangle & |b_1\rangle &= \hat{R}(\theta_b) |\alpha_1^B\rangle \\ |b'_0\rangle &= \hat{R}(\theta_{b'}) |\alpha_0^B\rangle & |b'_1\rangle &= \hat{R}(\theta_{b'}) |\alpha_1^B\rangle \end{aligned} \quad (23)$$

For the maximum Bell violation we choose $[\theta_a, \theta_{a'}, \theta_b, \theta_{b'}] = [0^\circ, 45^\circ, 22.5^\circ, 67.5^\circ]$. The CHSH correlation function encodes the $|0\rangle$ and $|1\rangle$ states with a -1 and $+1$ respectively. We define projection operators for measuring the four combinations of ± 1 , for measurements using the \mathbf{a} and \mathbf{b} bases.

$$\begin{aligned} \hat{P}_{--}(a, b) &= |a_0\rangle \langle a_0| \otimes |b_0\rangle \langle b_0| \\ \hat{P}_{-+}(a, b) &= |a_0\rangle \langle a_0| \otimes |b_1\rangle \langle b_1| \\ \hat{P}_{+-}(a, b) &= |a_1\rangle \langle a_1| \otimes |b_0\rangle \langle b_0| \\ \hat{P}_{++}(a, b) &= |a_1\rangle \langle a_1| \otimes |b_1\rangle \langle b_1| \end{aligned} \quad (24)$$

The expectation value for the product of the measurements (± 1) on A and B using these bases is then given by

$$\begin{aligned} \hat{P}_\times(a, b) &= P_{++}(a, b) - P_{+-}(a, b) \\ &\quad - P_{-+}(a, b) + P_{--}(a, b) \end{aligned} \quad (25)$$

$$E(a, b) = \langle P_\times \rangle = \text{Tr}(\hat{\rho} \hat{P}_\times(a, b)). \quad (26)$$

Expressions analogous to Eq.(24) and (26) define similar quantities $E(a, b')$, $E(a', b)$, and $E(a', b')$ using the other choices of basis states. The CHSH correlation function is then defined to be

$$S_{\text{CHSH}} = |E(a, b) - E(a, b') + E(a', b) + E(a', b')|. \quad (27)$$

The assumption of local realism yields the Bell inequality

$$S_{\text{CHSH}} \leq 2. \quad (28)$$

For local values of a, a', b , and b' which are distributed randomly and uniformly $S_{\text{CHSH}} = \sqrt{2}$, obeying the inequality. For the fully entangled Bell state of Eq. (13), by contrast, $S_{\text{CHSH}} = 2\sqrt{2}$, in violation of (28).

Starting with the initial state shown in Eq. (16), we solve for the unitary evolution of the global density matrix using Eq. (12) and calculate the correlation functions $S_{\text{Mermin}}(t)$ and $S_{\text{CHSH}}(t)$ directly from the global density matrix. The number of environmental double-dots is $N_E = 10$ (five around each target double-dot) yielding $2^{10} = 1024$ environmental electronic configurations. The results are shown in Fig. (2) for $a = 1$ nm, a typical scale for molecular double-dots (this sets the time scale at fs). Calculated Bell correlation functions are shown for four different values of R/a , corresponding to different average strengths of coupling to the environment (line colors). For each value of R/a , 12 different random geometric arrangements of the environments are shown. The CHSH correlation function $S_{\text{CHSH}}(t)$ for each of these 48 configurations, shown on the upper part of the figure, begins at the fully quantum entangled Bell-violating value and decreases, dropping out of the Bell violation regime and decaying to the classical limit. The Mermin correlation behaves similarly, crossing out of the Bell violation regime and rising to the classical (local realism) limit. For each specific environmental geometry, the crossover out of the Bell violation regime occurs at approximately the same time for both correlation function measures. As expected, the stronger the coupling to the environment, the faster the quantum entanglement disappears.

Fig. (3) shows exactly the same 48 cases of the geometrically random environment as Fig. (2), but plotted on a time axis scaled by the characteristic time τ_E as calculated from Eq. (10). The value of τ_E is distinct for each of the random geometries of the environment. The time-scaled result is independent of the values of a or R/a . The dots show the value of a single Gaussian fit to all 48 curves for the transition from the initial Bell-state value to the classical limit. The fit yields a Gaussian width of $\tau_{\text{opt}} = 1.34 \tau_E$. We conclude that both correlation functions evolve from their fully entangled value to the value corresponding to local realism over a time on the scale of τ_E and that the transition is very close to Gaussian, rather than the often-assumed exponential associated with semigroup behavior. The slope at small times is here zero.

A similar Gaussian characteristic has been observed by Cucchietti *et al.* [13] in the context of the decoherence of a model spin system. This result holds across many distributions of coupling to the environment and is rooted in the approximately Gaussian distribution of the eigenvalues of the Hamiltonian for a random environment. We predict similar behavior in the loss of entanglement driven by the effect of the environments on the A and B systems.

Disentanglement can be distinguished from decoher-

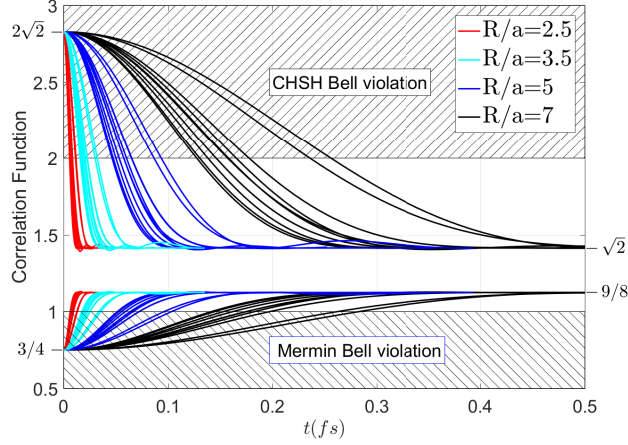


FIG. 2. Bell correlation functions measure the loss of entanglement under unitary evolution. A pair of double-dots start in a fully-entangled Bell state given by Eq.(13) and each subsequently interacts Coulombically with a different random local environment of similar double-dots, as shown in Fig. (1). The CHSH correlation function $S_{\text{CHSH}}(t)$ (top) and Mermin correlation function $S_{\text{Mermin}}(t)$ (bottom), defined by equations (21) and (27), are calculated as functions of time, assuming unitary evolution of the global system. The curves are shown for $a = 1$ nm (which sets the time-scale) and for 4 different values of R/a , corresponding to different average strengths of interaction with the environment. For each value of R/a , the results for 12 different random geometrical configurations of the environment are shown. The values of each correlation function for the pure entangled Bell state and for the (classical) case assuming local realism are shown on the left and right edges of the plot.

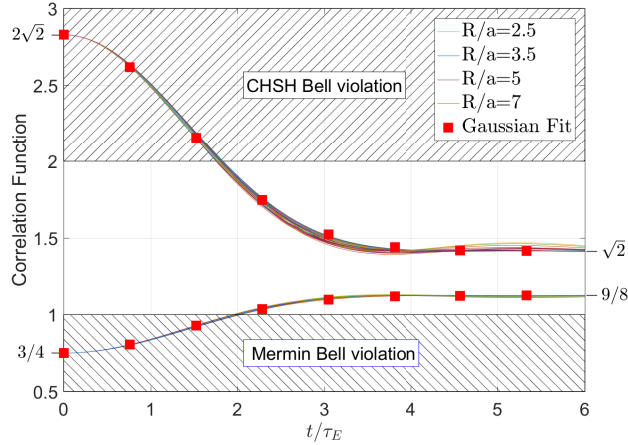


FIG. 3. Universal scaling of the CHSH and Mermin Bell correlation functions for different random geometries of the environment. The correlation functions for all 48 different geometrical configurations of the environment shown in Figure (2) are plotted here versus the time scaled by the characteristic time τ_E calculated from Eq. (10). The time τ_E is different for each random geometry. The points (squares) show the result of a Gaussian fit with characteristic time $\tau_{\text{opt}} = 1.34 \tau_E$.

ence. The loss of *entanglement*, as characterized by these Bell correlation functions, is a feature of the unitary evolution of the pure global quantum system—the environment E and the system cells AB . *Decoherence* by contrast, is the loss of *local* information about the system as it entangles with many environmental degrees of freedom. The von Neumann entropy of the global density matrix $\hat{\rho}(t)$ is zero at all times, while the entropy of the reduced density matrix, $\hat{\rho}^{AB}(t) = \text{Tr}_E \hat{\rho}$, goes from 0 to 1 on the timescale of τ_E . The off-diagonal elements of the reduced density matrix decay, but the off-diagonal elements of the full global density matrix do not—no information is lost or discarded.

Quantum entanglement is best characterized not as fragile, but rather as promiscuous. Dynamics entangles each system with all the other systems with which it interacts. This promiscuity is constrained by the principle of the quantum monogamy of entanglement [14, 15], which bounds the strength of entanglement between any two pairs when a system entangles with many other systems.

The model system we explore here shows how classical disentangled, but still correlated, states emerge in time from the fully entangled Bell states through completely unitary evolution. The time scale of disentanglement is τ_E which can be calculated precisely from the interaction with the environmental degrees of freedom.

Quantum indeterminism and the question of outcomes, of course, remain. Even in the long time limit with a large environment, the probability of measuring either subsystem A or B in the 1 state is $1/2$. Unitary interaction with the environment does not determine outcomes. Only a measurement event, whatever that entails, forces the physical world to make a “choice” between two open possibilities. Classical correlations also persist into the indefinite future. The probability of measuring A and B in opposite states remains 0 throughout. The enduring classical correlations are of the ordinary “Bertlemann’s socks” [16] variety.

* <http://www.nd.edu/~lent>; lent@nd.edu

- [1] A. Einstein, B. Podolsky, and N. Rosen, Phys. Rev. **47**, 777 (1935).
- [2] J. Bell, Physics **1**, 195 (1964).
- [3] M. Giustina, M. A. M. Versteegh, S. Wengerowsky, J. Handsteiner, A. Hochrainer, K. Phelan, F. Steinlechner, J. Kofler, J.-A. Larsson, C. Abellán, W. Amaya, V. Pruneri, M. W. Mitchell, J. Beyer, T. Gerrits, A. E. Lita, L. K. Shalm, S. W. Nam, T. Scheidl, R. Ursin, B. Wittmann, and A. Zeilinger, Phys. Rev. Lett. **115**, 250401 (2015).
- [4] L. K. Shalm, E. Meyer-Scott, B. G. Christensen, P. Bierhorst, M. A. Wayne, M. J. Stevens, T. Gerrits, S. Glancy, D. R. Hamel, M. S. Allman, K. J. Coakley, S. D. Dyer, C. Hodge, A. E. Lita, V. B. Verma, C. Lam-

- brocco, E. Tortorici, A. L. Migdall, Y. Zhang, D. R. Kumor, W. H. Farr, F. Marsili, M. D. Shaw, J. A. Stern, C. Abellán, W. Amaya, V. Pruneri, T. Jennewein, M. W. Mitchell, P. G. Kwiat, J. C. Bienfang, R. P. Mirin, E. Knill, and S. W. Nam, *Phys. Rev. Lett.* **115**, 250402 (2015).
- [5] B. Hensen, H. Bernien, A. Dréau, A. Reiserer, N. Kalb, M. Blok, J. Ruitenbergh, R. Vermeulen, R. Schouten, C. Abellán, *et al.*, *Nature* **526**, 682 (2015).
- [6] J. Handsteiner, A. S. Friedman, D. Rauch, J. Gallicchio, B. Liu, H. Hosp, J. Kofler, D. Bricher, M. Fink, C. Leung, *et al.*, *Phys. Rev. Lett.* **118**, 060401 (2017).
- [7] W. H. Zurek, *Rev. Mod. Phys.* **75**, 715 (2003).
- [8] E. P. Blair and C. S. Lent, *J. Appl. Phys.* **113**, 124302 (2013).
- [9] N. D. Mermin, *Phys. Today* **38**, 38 (1985).
- [10] L. Maccone, *Am. J. Phys.* **81**, 854 (2013).
- [11] J. F. Clauser, M. A. Horne, A. Shimony, and R. A. Holt, *Phys. Rev. Lett.* **23**, 880 (1969).
- [12] E. P. Blair, S. A. Corcelli, and C. S. Lent, *J. Chem. Phys.* **145**, 014307 (2016).
- [13] F. M. Cucchietti, J. P. Paz, and W. H. Zurek, *Phys. Rev. A* **72**, 052113 (2005).
- [14] V. Coffman, J. Kundu, and W. K. Wootters, *Phys. Rev. A* **61**, 052306 (2000).
- [15] T. J. Osborne and F. Verstraete, *Physical review letters* **96**, 220503 (2006).
- [16] J. S. Bell, in *Speakable and Unsayable in Quantum Mechanics* (Cambridge University Press, 2004) pp. 139–158.